Post-dissociation dynamics of N₂ on Ru(1000): How far can the "hot" N atoms travel?

Yingqi Wang and Hua Guo*

Department of Chemistry and Chemical Biology, University of New Mexico, Albuquerque, New Mexico 87131

^{*:} corresponding author, hguo@unm.edu

Abstract

Due to the high barrier and large exoergicity, the dissociation of N₂ impinging on Ru(0001) produces ballistic N atoms that can travel significant distances from the impact site, as shown by a recent STM study (*J. Phys. Chem. C* 2022, *126*, 18333-18342). In this work, the "hot" nitrogen atom dynamics following N₂ dissociation is investigated theoretically on a high-dimensional potential energy surface based on a neural network representation of density functional theory data. Quasi-classical trajectory simulations indicate that the average separation between the two N atoms is typically less than 10 Å, about one order of magnitude less than the experimental report (66±28 Å). The relatively short migration distance of the "hot" N atom found in our simulations is attributed to a high diffusion barrier and fast energy dissipation. The theory-experiment discrepancy presents a challenge to quantitative understanding "hot" atom dynamics on metal surfaces.

I. Introduction

The dissociative chemisorption of the N₂ molecule on catalytic surfaces is the rate-limiting step in the Haber-Bosch catalytic synthesis of ammonia¹ and has as a result attracted much attention.²⁻³ Ruthenium is considered as a second generation catalyst for this important reaction⁴⁻⁵ and its catalysis of ammonia synthesis has been extensively studied.⁶⁻¹⁶ In particular, N₂ dissociation is confirmed as the rate-limiting step on Ru surfaces.¹² As a result, experimental and theoretical studies of N₂ interaction and reaction with Ru surfaces have so far focused on the highly activated dissociative chemisorption,¹⁷⁻³⁰ but the dynamics after the initial dissociation is seldom investigated. Thanks to the high barrier and large exoergicity of the dissociation process, the resulting "hot" nitrogen atoms acquire significant kinetic energy from the breaking of the triple bond in the molecule, and are thus mobile on the metal surface immediately after the dissociation. The kinetic energy of these "hot" surface atoms might play a role in the subsequent N* + H* reaction step, which has a barrier of ~1 eV.¹¹⁻¹²

The thermal mobility of adsorbed N atoms on Ru surfaces has been investigated near room temperature using scanning tunneling microscopy (STM), which offers insights on the diffusion barrier. The surface temperature and coworkers reported an *in situ* STM study, in which the consequence of "hot" N atoms dynamics upon dissociative chemisorption of N₂ is probed on Ru(0001). At the surface temperature of 262 K, these authors observed clear N-N pairs on the surface, separated by an average of 66±28 Å, which does not change at room temperature. The large separation was attributed to the excess kinetic energy of the N atoms acquired after the dissociation, which is eventually dissipated into the substrate. Such dissipation could be due to energy exchange with the surface phonons and in some cases electron-hole pairs (EHPs) when the surface is a metal. The former is called the adiabatic dissipation channel because no excitation of

the metal electrons is involved, while the latter the nonadiabatic dissipation channel due to the strong coupling between the electronic and nuclear degrees of freedom. They often have very different behaviors and the understanding of their roles in surface processes is a hot topic in surface dynamics.³⁴⁻³⁶ For our system here, an accurate characterization of the energy dissipation is the key to understanding the experimental observations. Here, we report an extensive theoretical investigation of the N₂ dissociative chemisorption on Ru(0001) and the subsequent "hot" N atom dynamics, using an approach adapted in our recent work on hydrogen spillover.³⁷⁻³⁸

II. Methods

Periodic density functional theory (DFT) calculations reported in this paper were carried out using the Vienna Ab initio Simulation Package (VASP).³⁹⁻⁴⁰ The valence electrons were represented by plane waves with an energy cutoff of 400 eV and the projector-augmented wave (PAW) method was applied to account for the core electrons.⁴¹ The exchange and correlation energies were described within the generalized gradient approximation (GGA) by the revised Perdew-Burke-Ernzerhof (RPBE) functional,⁸ which has been widely employed in many previous studies for the same system.^{13, 25, 28} In the calculations, the Ru(0001) surface was modeled by a 4×4 unit cell with 4 layers, with sixty four atoms. The Brillouin zone was sampled with a $2\times2\times1$ k-point grid. The slabs were separated by a vacuum space of 16 Å in the z direction. All atoms other than those in the bottom surface layer were allowed to move. The self-consistent field calculations were converged to 10^{-5} eV.

The calculation of adsorption energy was based on the equation below,

$$E_{\text{ad}}(\text{adsorbate}) = E(\text{surface+adsorbate}) - E(\text{surface}) - E(\text{adsorbate})$$
 (1)

where E(surface), E(adsorbate), and E(surface+adsorbate) are the energy of the bare surface, the adsorbate in gas phase, and the total system, respectively. The saddle points were determined using the climbing image-nudged elastic band (CI-NEB) method⁴² with the force convergence criterium of 0.05 eV/Å per atom.

Because of the high activation barrier for dissociation, the impinging N_2 needs to have a large internal energy and/or kinetic energy to have a significant sticking probability. To generate DFT data points for constructing the potential energy surface (PES), ab initio molecular dynamics (AIMD) trajectories were run for N_2 molecules with the incidence energy of 5.0 eV and incidence angle along surface normal. The internal energy of the impinging molecule was sampled in the v=4 state with zero rotational angular momentum. The surface temperature was set at 300 K, and the initial surface configurations were saved from a 1-ps equilibration run. The initial position of the N_2 molecule was evenly distributed over the surface unit cell at 6 Å above and their polar and azimuthal angles are randomly selected. 400 trajectories were run for 0.5 ps with a 0.5 fs time step, among which 137 resulted in dissociation.

The AIMD data were then used to construct a high-dimensional PES for N₂ interacting with Ru(0001) using a machine learning method. ⁴³⁻⁴⁴ The PES is expressed as an atomistic neural network (AtNN), in which the total interaction energy is given as a sum of atomic contributions. ⁴⁵⁻⁴⁶ A total of 48 surface atoms and two N atoms are included and the dimensionality of the PES is 150. Specifically, the embedded atom neural network (EANN) approach was used, which is known to be more efficient than previous AtNN methods. ⁴⁸ The training data set consisted of points (both energies and gradients) along the AIMD trajectories, which were culled using a Euclidean distance of 0.3 Å to remove points that were too close to each other. An additional 6000 points were added to cover configuration spaces that are not accessed by the limited number of

trajectories. About 50000 points were finally used to fit the PES, with a fitting root mean square error (RMSE) of about 37 meV, which is 0.74 meV/atom. To verify the fidelity of the fitting, the potential energies along an AIMD dissociative trajectory are compared with the values obtained from the PES in Supporting Information (SI), and the comparison is quite satisfactory.

With the PES, the dissociation of N₂ and subsequent impulsive dynamics of N atoms were simulated using quasi-classical trajectories (QCT). The assumption that the dynamics is classical is reasonable as the nuclei involved are all quite heavy. The propagation of the trajectories was done with a 0.1 fs time step. A trajectory is terminated if the molecule is scattered back to the gas phase, judged by the center-of-mass distance from the surface larger than 6 Å. Other trajectories are propagated to 20 ps, although some to 200 ps in order to check convergence. The trajectories were calculated using the Venus program⁴⁹ with modifications for surface processes.⁵⁰ Several incidence energies and N₂ vibrational excitations were used to prepare the hot N atoms on the surface.

The EHP effects are not considered in the present work because an earlier study has demonstrated that the nonadiabatic coupling of atomic nitrogen with the surface EHPs is small on metal surfaces.²⁷

III. Results

IIA. N adsorption, diffusion, and N₂ dissociation

Previous theoretical studies indicated that the N atom prefers three-fold hollow sites of the Ru(0001) surface, ^{7, 11-12, 15, 51} which has been confirmed by STM experiments. ³²⁻³³ The distance of the N adsorbate from the surface plane is 1.08 and 1.19 Å for hcp and fcc sites, respectively. Our calculations show that N adsorbs stronger at the hcp site than the fcc site by about 0.49 eV, and

their configurations are shown in Figure 1. The adsorption energy relative to the gaseous nitrogen atom is -5.59 and -5.10 eV, respectively. For an N atom to move from the most stable hcp site to the less stable fcc site, it needs to overcome a diffusion barrier of 0.85 eV. STM experiments by Ertl and coworkers estimated that the N atom diffusion barrier on Ru(0001) is 0.94 eV,³¹ which is comparable to our results. Previous theoretical calculations also gave similar values around 0.8-1.0 eV under different coverages of N adsorption.^{7, 15, 51}

For dissociation on the Ru(0001) surface, the N₂ molecule first physisorbs perpendicular to the surface with an adsorption energy of ~0.3 eV. The N-N bond length in this state is about 1.13 Å, which is about the same as that in the isolated N₂ molecule. The dissociation transition state adapts a configuration parallel to the surface where one N atom stays near an fcc site and the other near an hcp site, with a N-N distance of about 1.69 Å. In the final state, the N atoms occupy two adjacent hcp sites. The configurations of the stationary points for N₂ dissociation and N atom diffusion are shown in Figure 1. The barrier for N₂ dissociation (TS1) on Ru(0001) is calculated to be ~1.84 eV from the physisorption well (MIN1), consistent with previously reported DFT values of 1.80⁷ and 1.84 eV.²⁸ Relative to the dissociation asymptote, the barrier is 1.54 eV. The dissociation reaction has an exoergicity of 0.96 eV. The diffusion barrier (TS2) is 0.85 eV from hcp (MIN2) to fcc (MIN3), which is 0.49 eV higher in energy.

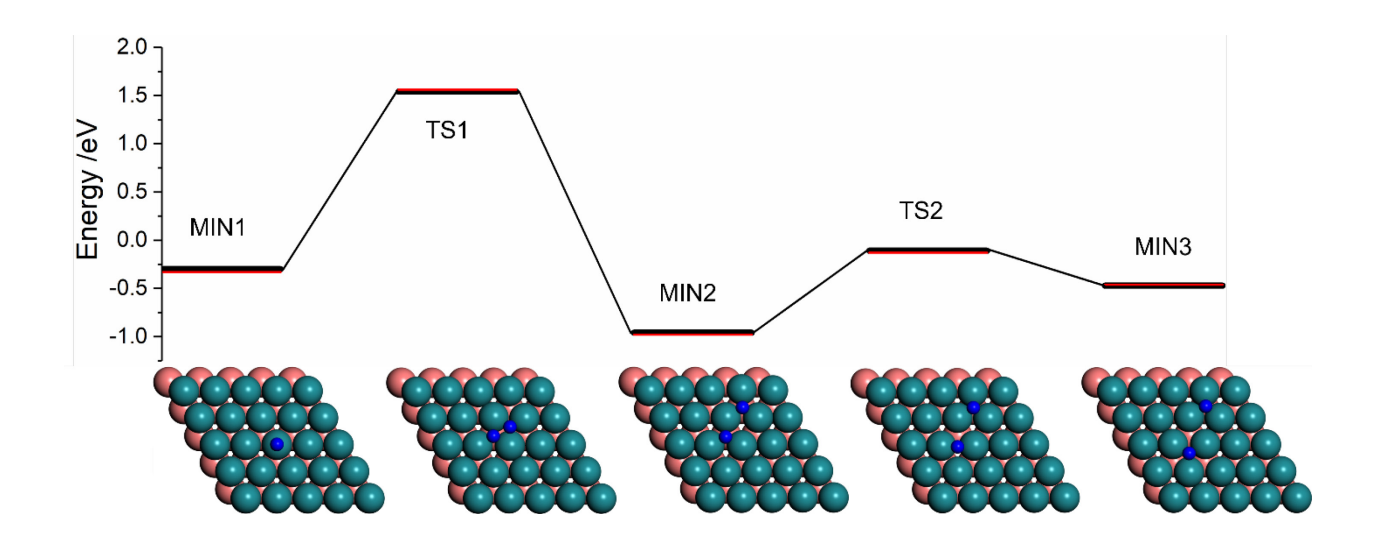


Figure 1. Energy diagram for the dissociation of N_2 and subsequent diffusion of N atoms on the Ru(0001) surface, with the top view of stationary points. The black lines are DFT values while the red lines are those from PES. The nitrogen, top layer Ru and sublayer Ru atoms are colored as blue, green, and pink, respectively.

IIIB. Dynamics simulations: N₂ dissociation and N diffusion

QCT simulations of N_2 dissociation and the subsequent diffusion of newly generated N atoms were carried out on the DFT based EANN PES. Starting from 6 Å above the surface with random initial orientations, most of the impinging N_2 molecules scatter back to the gas phase immediately or after a short residence time on the surface, due apparently to the high activation barrier, while some undergo dissociation. The experimental supersonic beam conditions described by Wagner et al.³³ were characterized using time-of-flight measurements to have incident beam energies of 0.8 ± 0.3 , 1.1 ± 0.4 , and 1.3 ± 0.6 eV that were achieved using nozzle temperatures of 730, 1000, and 1150 K, respectively. Significant vibrational excitation of the N_2 molecule is thought to exist under the experimental conditions. As a result, we have performed three sets of calculations with incidence energy of 1.0 and 5.0 eV for impinging N_2 with v=2 and 4. Table I lists the total number of trajectories calculated and fraction of dissociation under these initial conditions. At the low

incidence energy at 1.0 eV, the dissociation probability for $N_2(v=2)$ on the order of 10^{-4} is consistent with experimental observations. The dissociation fraction increases with both kinetic and vibrational excitations, also consistent with previous observations. 18, 21, 25-26, 28

Table 1. Number of trajectories and dissociation probability at different initial conditions.

	$E_{\rm i} = 1 {\rm eV}, \nu = 2$	$E_{\rm i} = 1 {\rm eV}, {\rm v} = 4$	$E_{\rm i} = 5 {\rm eV}, {\rm v} = 2$
Total number of trajectories	500000	20000	5000
Fraction of dissociation	0.0004	0.02	0.3

After N_2 is dissociated, the excess kinetic energy leads to hyperthermal motions of N atoms. Measuring from the dissociation barrier, the total available energy for the two nitrogen atoms is ~ 2.50 eV, resulting from the sum of the barrier (1.54 eV) and the 0.96 eV exoergicity of the reaction. Additional energy is provided by the vibrational and translational degrees of freedom of the impinging N_2 . The energy is insufficient for atomic N to desorb, but can lead to "hot" N atoms. The QCT simulation with an N_2 incidence translation energy of 1.0 eV and vibrational excitation v=2 at surface temperature of 300 K has a dissociation probability of 0.04 %. After the system achieved equilibration, the average separation between two adsorbed N atoms is ~ 4.3 Å with the largest separation of ~ 7.4 Å. The corresponding distribution of the N-N separation is shown in the upper panel of Figure 2. The diffusion of the "hot" N atom does not seem to have any preference of directionality, as evidenced by the angular distribution of the diffusion shown in the lower panel of Figure 2, which is consistent with the experimental observations.³³

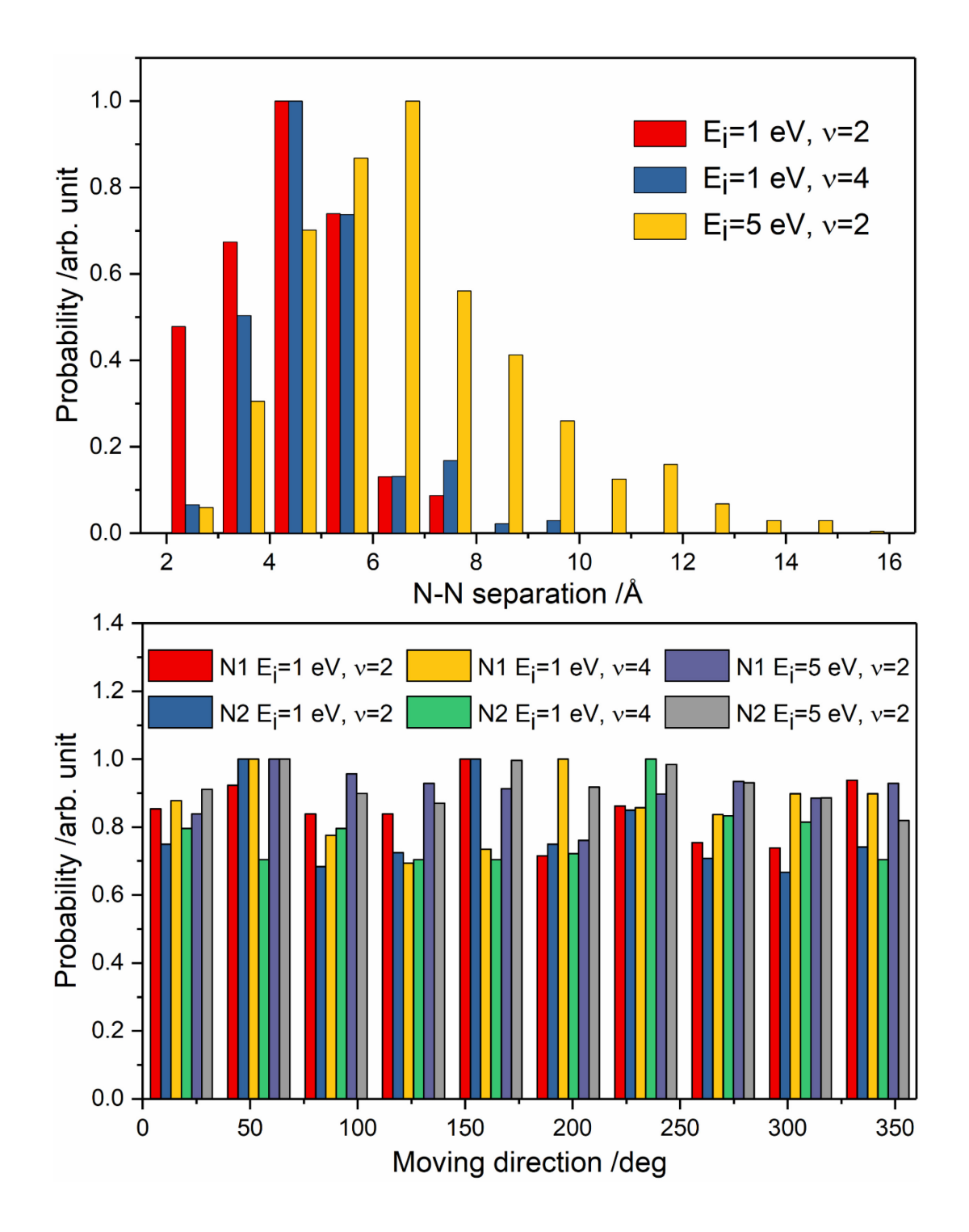


Figure 2. The distribution of N-N separation at different initial conditions (upper panel). The angular distribution of two N atoms after dissociation (lower panel).

To find out how vibrational excitation of the incident N_2 affects the dissociation and diffusion, trajectories were also run with v=4 at the incident energy of 1.0 eV. As shown in Table 1, the vibrational excitation clearly promotes the dissociation, leading to a dissociation probability of 2%. This is readily understood as the N-N vibration is well aligned with the reaction coordinate at the dissociation saddle point, in the language of the Sudden Vector Projection model.⁵² However, the overall N-N separation distribution shown in Figure 2 changes only moderately, resulting in average and maximum N-N distances of 4.9 and 9.7 Å, respectively.

Similarly, when the initial translational energy of N_2 molecule was increased to 5.0 eV while the N_2 vibrational state is kept at v=2, the dissociation probability also increases. Again, the drastically increased energy in the impinging N_2 has only a limited effect on the N-N separation, as shown in Figure 2. The average and maximum N-N separations are 6.8 and 16.2 Å, respectively. The larger separations can be attributed to the higher incidence energy, which is much larger than the energy imparted by vibrational excitation (0.6 eV between the v=2 and v=4 vibrational levels of N_2).

The N atom that is placed at the hcp site from the N₂ dissociation typically does not have significant movement. On the other hand, the one at the fcc site at the transition state is more likely to travel, across one or two Ru surface lattice units (2.7 Å). This behavior is quite similar to the "hot" H dynamics after the dissociation of H₂.^{37-38,53} In Figure 3, the N-N separation averaged over all the dissociated trajectories is shown as a function of time. Higher energy trajectories typically lead to larger N-N separations, consistent with the results shown in Figure 2. It is clear that the impulsive motion is essentially finished after 2 ps, due apparently to strong energy dissipation to surface phonons, although the N atoms still possess some kinetic energy. The average N-N separation in these three simulations is 4.3, 4.9, and 6.8 Å. In Figure 4, an exemplary trajectory is

shown, where the motion of the "hot" N atom (yellow) is via hopping between hollow sites via the bridge diffusion transition state, while the other N atom (purple) is trapped at the initial hcp site.

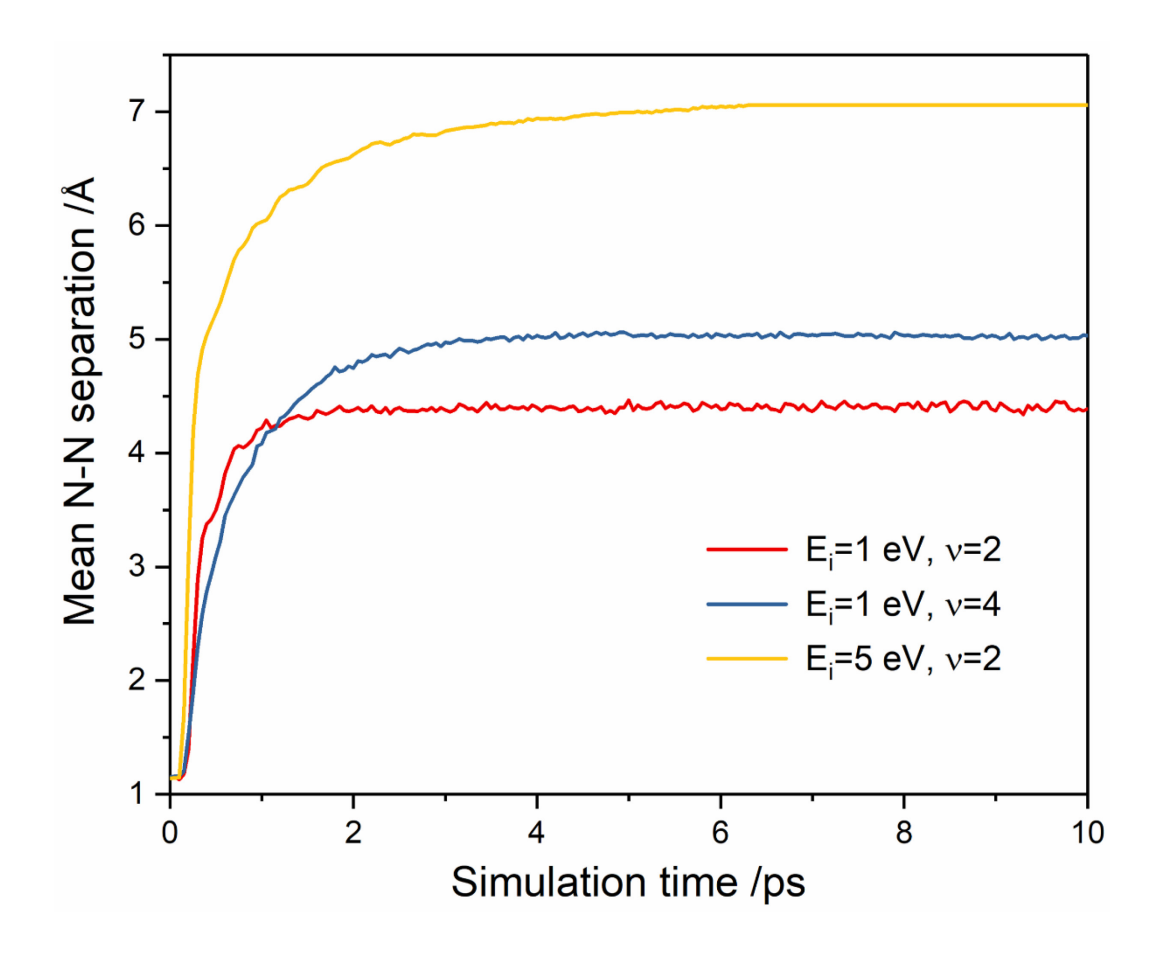


Figure 3. Mean N-N distances as a function of simulation time for several initial conditions.

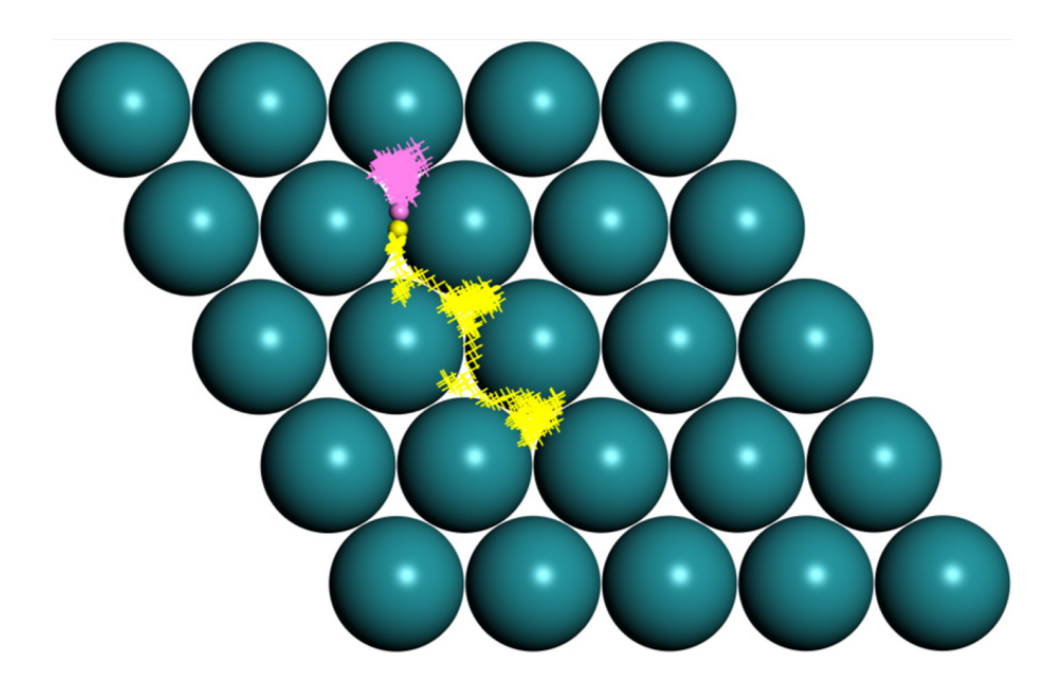


Figure 4. An exemplary trajectory at the incidence energy of 1.0 eV with $N_2(\nu=2)$. The two N atoms are represented by different colors. The solid red dot depicts the initial position of N_2 in the surface unit cell.

One dominant factor that prevents "hot" N atoms from longer distance movement is their strong coupling with the Ru(0001) surface. The kinetic energy of the N atoms quickly decreases after dissociation because of fast dissipation to the surface phonons. As shown above, the "hot" atom diffusion is essentially done within the first 2 ps after dissociation, after which the N atoms are trapped around the adsorption site. Thermal diffusion is too slow for the QCT simulation to capture. Figure 5 presents the kinetic energy of two N atoms parallel (X+Y) and perpendicular (Z) to the surface as a function of time, following the same trajectory shown in Figure 4. The trajectory reaches TS1 around 0.2 ps, after which there is a significant increase in kinetic energy due to the dissociation. For this particular trajectory, a major part of the energy release goes to the translational energy in a direction parallel to the surface for in one N atom, which reaches as high

as 0.7 eV. However, the kinetic energy quickly declines to below 0.3 eV, losing the capacity to move further on the surface. The decrease of the lateral kinetic energy near 0.6 ps is accompanied by an increase of kinetic energy in the Z direction, suggesting energy transfer due to the strong corrugation of the surface. The subsequent energy loss near 1.2 ps is apparently due to the surmounting of the diffusion transition state (TS2) and further energy loss to the surface.

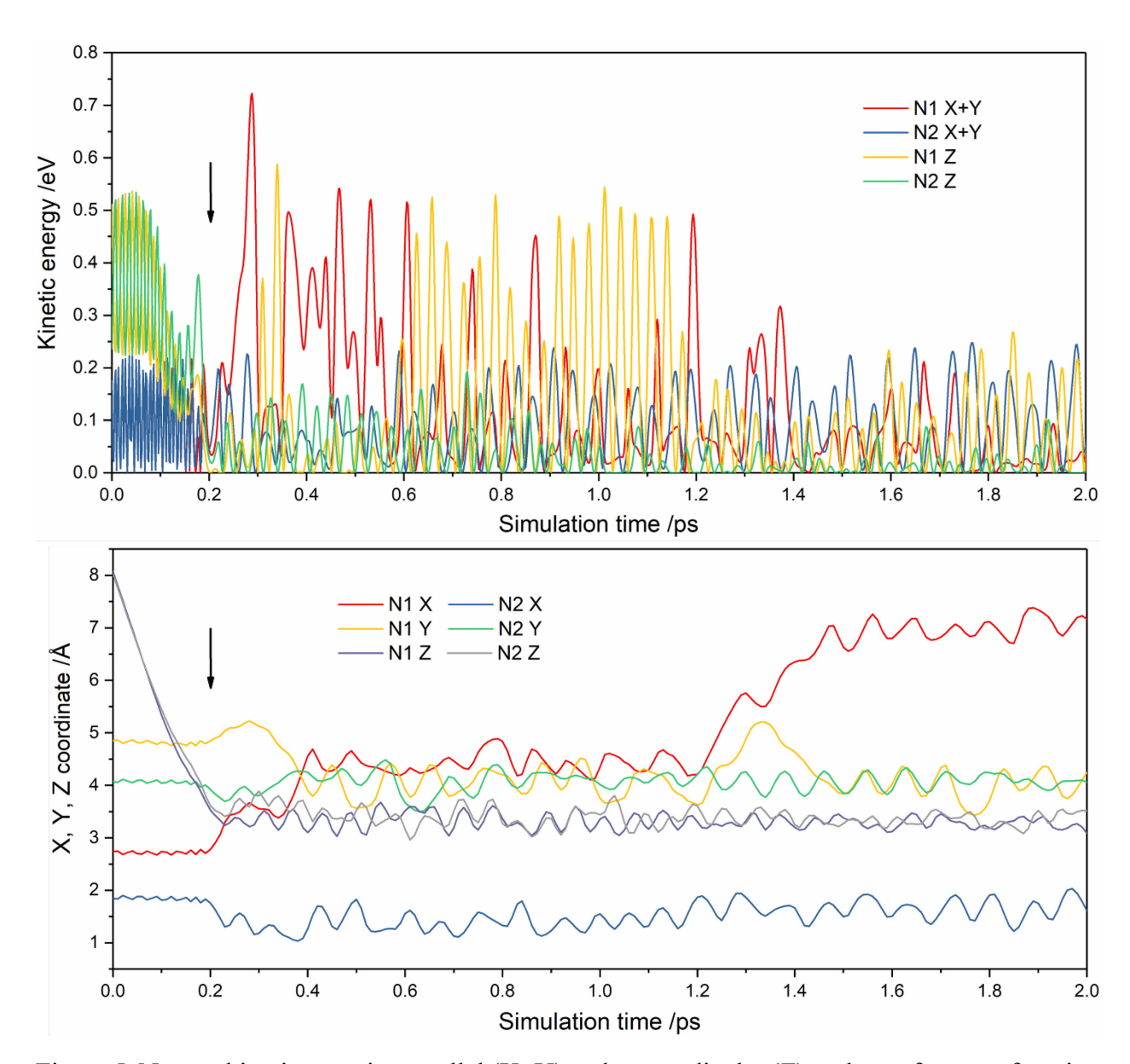


Figure 5. N atom kinetic energies parallel (X+Y) and perpendicular (Z) to the surface as a function of time for an exemplary trajectory (upper panel). The corresponding X, Y, Z coordinates of the

two N atoms are shown in the lower panel. The dissociation occurring at 0.2 ps is indicated by an arrow.

IV. Discussion

It is quite clear that our simulation results are inconsistent with the observations made in the careful experiments by Sibener and coworkers.³³ The difference in N-N separation is by approximately one order of magnitude (Å vs. nm). Since the incident experimental beam energy distributions were not monoenergetic and had uncharacterized N₂ vibrational excitation, we have performed three different combinations of initial conditions. The total energies in our simulations are probably larger than the ones in the experiment, but this was intentional, as lower total energies are expected to further reduce the final N-N separation. Yet, the increase of either the incidence translational energy or internal vibrational energy failed to achieve even a qualitative reproduction of experiment.

A possible source of errors is the uncertainty associated with the density functional used in our simulation. However, our calculated diffusion barrier 0f 0.85 eV is similar to earlier DFT values of 0.8-1.0 eV using GGA functionals.^{7, 15, 51} More importantly, the calculated barrier is in good agreement with earlier experiments by Ertl and coworkers, who estimated the diffusion activation energy to be 0.94 eV.³¹

One might argue that the neglect of the EHPs in our simulations could be the culprit for the disagreement. However, it is well established that EHP excitations in the substrate typically serves as a friction to the diffusing adsorbate. Indeed, our recent work on H spillover had shown that interactions with substrate EHPs significantly slow down the diffusion of adsorbed H atoms, leading to smaller diffusion coefficients than those obtained via adiabatic simulations.³⁷⁻³⁸

However, previous studies on N diffusion on metal surfaces have demonstrated that the nonadiabatic friction is typically minor.²⁷ Even if the electronic friction were to be included in our simulation, it can be expected that the final N-N separation will be even smaller.

Another potential shortcoming of our model is the relatively small size of the unit cell. There is evidence that the limited size of the unit cell may result in insufficient energy dissipation due to the missing low frequency phonons.⁵⁴⁻⁵⁷ However, a large unit cell, which is numerically more expensive to simulate, would inevitably lead to more dissipation of the N kinetic energy, thus leading to shorter N-N distance.

It might be profitable to compare "hot" N atoms with "hot" O atoms generated from dissociation of O₂ on various metal surfaces. STM studies have revealed that after the cleavage of the O-O bond, the "hot" O atoms typically travels for less than or near 10 Å on low Miller index facets of metals, including Pt(111),⁵⁸ Cu(110),⁵⁹ Rh(110),⁶⁰ Al(111),⁶¹ Pd(111),⁶² and Ag(110).⁶³ The only reported O-O separation significantly above this range was the earlier studies by Brune et al. on the Al(111) surface, where the "hot" O atoms are observed to reach separations at least 80 Å.⁶⁴⁻⁶⁵ However, this conclusion was challenged by the later experiment of Schmid et al.,⁶¹ who observed O-O pairs separated by only ~2-3 surface lattice distances (~5 Å). Another STM study observed O-O distances of a few nm was on Ag(001),⁶⁶ but no theoretical study has so far been reported. Comparing with N, the diffusion barrier for O atoms is much lower (~ 0.5 eV). This difference also argues against a larger separation of "hot" N atoms upon dissociation. Indeed, theoretical studies of the O diffusion on metal surfaces showed reasonable agreement with experiment, yielding O-O separation less than or around 10 Å.⁵⁴⁻⁵⁶, ⁶⁷⁻⁶⁹ We note in passing that the EHP friction of adsorbed O atoms in these cases is also known to be small.⁷⁰

Finally, we have examined the so-called "cannonball" mechanism, ⁷¹ in which one of the N atom is supposed to shoot away from the surface while the other towards the surface if N₂ has a non-zero angle to the surface when it reaches the dissociation barrier. As a result, the N atom pushed away from the surface might be able to travel long distances. As shown in SI, the N₂ dissociation barrier is highly anisotropic with respect to the polar angle of the impinging N₂, which results in strong steering of the molecule toward the saddle point with a configuration parallel to the surface even it is originally oriented at a different angle with the surface. This steering effect leads to very few trajectories with non-parallel orientations when N₂ reaches the dissociation barrier, and even for these trajectories, no long-distance hopping of N atom was observed.

To summarize, it is difficult to rationalize the large experiment-theory discrepancy in the N-N separation upon dissociation of N₂ on Ru(0001) by potential shortcomings of our theoretical model. Our results are mostly consistent with previous theoretical studies of "hot" atoms formed by dissociative chemisorption on metals. We thus conclude that the experimental observations must be the result of a yet-to-be-discovered mechanism that is not considered in our theoretical model. It is difficult at this point to speculate the origin except that the theoretical model used in this work is highly idealized, lacking features that cannot be avoided in reality such as surface defects.

V. Conclusions

Inspired by recent experimental work, 33 we constructed a high-dimensional PES for the dissociation of N_2 and the subsequent diffusion of the resulting hot N atoms on Ru(0001) based on DFT calculations. The final N-N separation distribution is obtained from QCT simulations on the PES for several initial conditions mimicking experimental conditions. The average separation is within 10 Å, due apparently to the strong energy dissipation of the "hot" N atoms and the high

diffusion barrier on the Ru(0001) surface that has been confirmed by another experiment. The theoretical N-N separation is significantly smaller than the 66±28 Å average separation reported in the experiment. After careful examination of the approximations used in our simulations, we conclude that the experimentally observed large N-N separation must be originated from a yet-unknown mechanism. The eventual understanding of this puzzle will open doors for other related systems in surface science.

Acknowledgments: This work was supported by NSF (Grant No. CHE-1951328). We thank Steve Sibener and Josh Wagner for sharing experimental results with us prior to publication and for many stimulating discussions. We also thank Prof. Bin Jiang and Prof. Geert-Jan Kroes for many useful discussions. The computations were performed at the Center for Advanced Research Computing (CARC) at UNM.

References:

- 1. Ertl, G., Reactions at Surfaces: From Atoms to Complexity (Nobel Lecture). *Angew. Chem. Int. Ed.* **2008**, *47*, 3524-3535.
- 2. Ertl, G., Primary Steps in Catalytic Synthesis of Ammonia. *J. Vac. Sci. Technol. A* **1983**, *1*, 1247-1253.
- 3. Nielsen, A., Ammonia: Catalysis and Manufacture. Springer: Berlin, 2012.
- 4. Aika, K.-i.; Hori, H.; Ozaki, A., Activation of Nitrogen by Alkali Metal Promoted Transition Metal I. Ammonia Synthesis over Ruthenium Promoted by Alkali Metal. *J. Catal.* **1972**, *27*, 424-431.
- 5. Hellman, A., et al., Predicting Catalysis: Understanding Ammonia Synthesis from First-Principles Calculations. *J. Phys. Chem. B* **2006**, *110*, 17719-17735.
- 6. Rosowski, F.; Hornung, A.; Hinrichsen, O.; Herein, D.; Muhler, M.; Ertl, G., Ruthenium Catalysts for Ammonia Synthesis at High Pressures: Preparation, Characterization, and Power-Law Kinetics. *Appl. Catal. A* **1997**, *151*, 443-460.
- 7. Mortensen, J. J.; Morikawa, Y.; Hammer, B.; Nørskov, J. K., Density Functional Calculations of N₂ Adsorption and Dissociation on a Ru(0001) Surface. *J. Catal.* **1997**, *169*, 85-92.
- 8. Hammer, B.; Hansen, L. B.; Nørskov, J. K., Improved Adsorption Energetics within Density Functional Theory Using Revised Perdew-Burke-Ernzerhof Functionals. *Phys. Rev. B* **1999**, *59*, 7413-7421.
- 9. Dahl, S.; Logadottir, A.; Egeberg, R. C.; Larsen, J. H.; Chorkendorff, I.; Tornqvist, E.; Nørskov, J. K., Role of Steps in N₂ Activation on Ru(0001). *Phys. Rev. Lett.* **1999**, *83*, 1814-1817.
- 10. Dahl, S.; Sehested, J.; Jacobsen, C. J. H.; Törnqvist, E.; Chorkendorff, I., Surface Science Based Microkinetic Analysis of Ammonia Synthesis over Ruthenium Catalysts. *J. Catal.* **2000**, *192*, 391-399.
- 11. Zhang, C. J.; Lynch, M.; Hu, P., A Density Functional Theory Study of Stepwise Addition Reactions in Ammonia Synthesis on Ru(0 0 0 1). *Surf. Sci.* **2002**, *496*, 221-230.
- 12. Logadóttir, Á.; Nørskov, J. K., Ammonia Synthesis over a Ru(0001) Surface Studied by Density Functional Calculations. *J. Catal.* **2003**, *220*, 273-279.
- 13. Honkala, K.; Hellman, A.; Remediakis, I. N.; Logadottir, A.; Carlsson, A.; Dahl, S.; Christensen, C. H.; Nørskov, J. K., Ammonia Synthesis from First-Principles Calculations. *Science* **2005**, *307*, 555-558.
- 14. van Harrevelt, R.; Honkala, K.; Nørskov, J. K.; Manthe, U., The Effect of Surface Relaxation on the N₂ Dissociation Rate on Stepped Ru: A Transition State Theory Study. *J. Chem. Phys.* **2006**, *124*, 026102.
- 15. Herron, J. A.; Tonelli, S.; Mavrikakis, M., Atomic and Molecular Adsorption on Ru(0001). *Surf. Sci.* **2013**, *614*, 64-74.
- 16. Lee, E. M. Y.; Ludwig, T.; Yu, B.; Singh, A. R.; Gygi, F.; Nørskov, J. K.; de Pablo, J. J., Neural Network Sampling of the Free Energy Landscape for Nitrogen Dissociation on Ruthenium. *J. Phys. Chem. Lett.* **2021**, *12*, 2954-2962.
- 17. Shi, H.; Jacobi, K.; Ertl, G., Dissociative Chemisorption of Nitrogen on Ru(0001). *J. Chem. Phys.* **1993**, *99*, 9248-9254.
- 18. Romm, L.; Katz, G.; Kosloff, R.; Asscher, M., Dissociative Chemisorption of N₂ on Ru(001) Enhanced by Vibrational and Kinetic Energy: Molecular Beam Experiments and Quantum Mechanical Calculations. *J. Phys. Chem. B* **1997**, *101*, 2213-2217.
- 19. Papageorgopoulos, D. C.; Berenbak, B.; Verwoest, M.; Riedmüller, B.; Stolte, S.; Kleyn, A. W., A Molecular Beam Study of the Scattering and Chemisorption Dynamics of N₂ on Ru(0001). *Chem. Phys. Lett.* **1999**, *305*, 401-407.
- 20. Romm, L.; Citri, O.; Kosloff, R.; Asscher, M., A Remarkable Heavy Atom Isotope Effect in the Dissociative Chemisorption of Nitrogen on Ru(001). *J. Chem. Phys.* **2000**, *112*, 8221-8224.
- 21. Diekhöner, L.; Mortensen, H.; Baurichter, A.; Jensen, E.; Petrunin, V. V.; Luntz, A. C., N₂ Dissociative Adsorption on Ru(0001): The Role of Energy Loss. *J. Chem. Phys.* **2001**, *115*, 9028-9035.

- 22. Egeberg, R. C.; Larsen, J. H.; Chorkendorff, I., Molecular Beam Study of N₂ Dissociation on Ru(0001). *Phys. Chem. Chem. Phys.* **2001**, *3*, 2007-2011.
- 23. Diekhöner, L.; Hornekær, L.; Mortensen, H.; Jensen, E.; Baurichter, A.; Petrunin, V. V.; Luntz, A. C., Indirect Evidence for Strong Nonadiabatic Coupling in N2 Associative Desorption from and Dissociative Adsorption on Ru(0001). *J. Chem. Phys.* **2002**, *117*, 5018-5030.
- 24. van Harrevelt, R.; Honkala, K.; Nørskov, J. K.; Manthe, U., The Reaction Rate for Dissociative Adsorption of N_2 on Stepped Ru(0001): Six-Dimensional Quantum Calculations. *J. Chem. Phys.* **2005**, *122*, 234702.
- 25. Díaz, C.; Vincent, J. K.; Krishnamohan, G. P.; Olsen, R. A.; Kroes, G. J.; Honkala, K.; Nørskov, J. K., Multidimensional Effects on Dissociation of N₂ on Ru(0001). *Phys. Rev. Lett.* **2006**, *96*, 096102.
- 26. Díaz, C.; Vincent, J. K.; Krishnamohan, G. P.; Olsen, R. A.; Kroes, G. J.; Honkala, K.; Nørskov, J. K., Reactive and Nonreactive Scattering of N₂ from Ru(0001): A Six-Dimensional Adiabatic Study. *J. Chem. Phys.* **2006**, *125*, 114706.
- 27. Martin-Gondre, L.; Alducin, M.; Bocan, G. A.; Díez Muiño, R.; Juaristi, J. I., Competition between Electron and Phonon Excitations in the Scattering of Nitrogen Atoms and Molecules Off Tungsten and Silver Metal Surfaces. *Phys. Rev. Lett.* **2012**, *108*, 096101.
- 28. Shakouri, K.; Behler, J.; Meyer, J.; Kroes, G.-J., Accurate Neural Network Description of Surface Phonons in Reactive Gas—Surface Dynamics: N₂ + Ru(0001). *J. Phys. Chem. Lett.* **2017**, *8*, 2131-2136.
- 29. Shakouri, K.; Behler, J.; Meyer, J.; Kroes, G.-J., Analysis of Energy Dissipation Channels in a Benchmark System of Activated Dissociation: N₂ on Ru(0001). *J. Phys. Chem. C* **2018**, *122*, 23470-23480.
- 30. Spiering, P.; Shakouri, K.; Behler, J.; Kroes, G.-J.; Meyer, J., Orbital-Dependent Electronic Friction Significantly Affects the Description of Reactive Scattering of N₂ from Ru(0001). *J. Phys. Chem. Lett.* **2019**, *10*, 2957-2962.
- 31. Zambelli, T.; Trost, J.; Wintterlin, J.; Ertl, G., Diffusion and Atomic Hopping of N Atoms on Ru(0001) Studied by Scanning Tunneling Microscopy. *Phys. Rev. Lett.* **1996**, *76*, 795-798.
- 32. Trost, J.; Zambelli, T.; Wintterlin, J.; Ertl, G., Adsorbate-Adsorbate Interactions from Statistical Analysis of Stm Images: N/Ru(0001). *Phys. Rev. B* **1996**, *54*, 17850-17857.
- 33. Wagner, J.; Grabnic, T.; Sibener, S. J., Stm Visualization of N₂ Dissociative Chemisorption on Ru(0001) at High Impinging Kinetic Energies. *J. Phys. Chem. C* **2022**, *126*, 18333-18342.
- 34. Rittmeyer, S. P.; Bukas, V. J.; Reuter, K., Energy Dissipation at Metal Surfaces. *Adv. Phys. X* **2018**, *3*, 1381574.
- 35. Alducin, M.; Díez Muiño, R.; Juaristi, J. I., Non-Adiabatic Effects in Elementary Reaction Processes at Metal Surfaces. *Prog. Surf. Sci.* **2017**, *92*, 317-340.
- 36. Jiang, B.; Guo, H., Dynamics in Reactions on Metal Surfaces: A Theoretical Perspective. *J. Chem. Phys.* **2019**, *150*, 180901.
- 37. Gu, K.; Wei, F.; Cai, Y.; Lin, S.; Guo, H., Dynamics of Initial Hydrogen Spillover from a Single Atom Platinum Active Site to the Cu(111) Host Surface: The Impact of Substrate Electron—Hole Pairs. *J. Phys. Chem. Lett.* **2021**, *12*, 8423-8429.
- 38. Gu, K.; Li, C.; Jiang, B.; Lin, S.; Guo, H., Short- and Long-Time Dynamics of Hydrogen Spillover from a Single Atom Platinum Active Site to the Cu(111) Host Surface. *J. Phys. Chem. C* **2022**, *126*, 17093-17101.
- 39. Kresse, G.; Furthmuller, J., Efficient Iterative Schemes for Ab Initio Total-Energy Calculations Using Plane Wave Basis Set. *Phys. Rev. B* **1996**, *54*, 11169-11186.
- 40. Kresse, G.; Furthmuller, J., Efficiency of Ab Initio Total Energy Calculations for Metals and Semiconductors Using Plane Wave Basis Set. *Comp. Mater. Sci.* **1996**, *6*, 15-50.
- 41. Blöchl, P. E., Projector Augmented-Wave Method. *Phys. Rev. B* **1994**, *50*, 17953-17979.
- 42. Henkelman, G.; Uberuaga, B. P.; Jónsson, H., A Climbing Image Nudged Elastic Band Method for Finding Saddle Points and Minimum Energy Paths. *J. Chem. Phys.* **2000**, *113*, 9901-9904.

- 43. Behler, J., Perspective: Machine Learning Potentials for Atomistic Simulations. *J. Chem. Phys.* **2016**, *145*, 170901.
- 44. Jiang, B.; Li, J.; Guo, H., High-Fidelity Potential Energy Surfaces for Gas Phase and Gas-Surface Scattering Processes from Machine Learning. *J. Phys. Chem. Lett.* **2020**, *11*, 5120-5131.
- 45. Behler, J.; Parrinello, M., Generalized Neural-Network Representation of High-Dimensional Potential-Energy Surfaces. *Phys. Rev. Lett.* **2007**, *98*, 146401.
- 46. Behler, J., Atom-Centered Symmetry Functions for Constructing High-Dimensional Neural Network Potentials. *J. Chem. Phys.* **2011**, *134*, 074106.
- 47. Zhang, Y.; Hu, C.; Jiang, B., Embedded Atom Neural Network Potentials: Efficient and Accurate Machine Learning with a Physically Inspired Representation. *J. Phys. Chem. Lett.* **2019**, *10*, 4962-4967.
- 48. Zhou, X.; Zhang, Y.; Yin, R.; Hu, C.; Jiang, B., Neural Network Representations for Studying Gas-Surface Reaction Dynamics: Beyond the Born-Oppenheimer Static Surface Approximation. *Chin. J. Chem.* **2021**, *39*, 2917-2930.
- 49. Hase, W. L., et al., Venus96: A General Chemical Dynamics Computer Program. *Quantum Chemistry Program Exchange Bulletin* **1996**, *16*, 671.
- 50. Jiang, B.; Guo, H., Dynamics of Water Dissociative Chemisorption on Ni(111): Effects of Impact Sites and Incident Angles. *Phys. Rev. Lett.* **2015**, *114*, 166101.
- 51. Hammer, B., Adsorption, Diffusion, and Dissociation of No, N and O on Flat and Stepped Ru(0001). *Surf. Sci.* **2000**, *459*, 323-348.
- 52. Guo, H.; Jiang, B., The Sudden Vector Projection Model for Reactivity: Mode Specificity and Bond Selectivity Made Simple. *Acc. Chem. Res.* **2014**, *47*, 3679-3685.
- 53. Ramos, M.; Martínez, A. E.; Busnengo, H. F., H₂ Dissociation on Individual Pd Atoms Deposited on Cu(111). *Phys. Chem. Chem. Phys.* **2012**, *14*, 303-310.
- 54. Meyer, J.; Reuter, K., Modeling Heat Dissipation at the Nanoscale: An Embedding Approach for Chemical Reaction Dynamics on Metal Surfaces. *Angew. Chem. Int. Ed.* **2014**, *53*, 4721-4724.
- 55. Bukas, V. J.; Reuter, K., Hot Adatom Diffusion Following Oxygen Dissociation on Pd(100) and Pd(111): A First-Principles Study of the Equilibration Dynamics of Exothermic Surface Reactions. *Phys. Rev. Lett.* **2016**, *117*, 146101.
- 56. Bukas, V. J.; Reuter, K., Phononic Dissipation During "Hot" Adatom Motion: A Qm/Me Study of O₂ Dissociation at Pd Surfaces. *J. Chem. Phys.* **2017**, *146*, 014702.
- 57. Hu, C.; Lin, Q.; Jiang, B.; Guo, H., Influence of Supercell Size on Gas-Surface Scattering: A Case Study of Co Scattering from Au(111). *Chem. Phys.* **2022**, *554*, 111423.
- 58. Wintterlin, J.; Schuster, R.; Ertl, G., Existence of a "Hot" Atom Mechanism for the Dissociation of O₂ on Pt(111). *Phys. Rev. Lett.* **1996**, *77*, 123-126.
- 59. Briner, B. G.; Doering, M.; Rust, H. P.; Bradshaw, A. M., Mobility and Trapping of Molecules During Oxygen Adsorption on Cu(110). *Phys. Rev. Lett.* **1997**, *78*, 1516-1519.
- 60. Hla, S. W.; Lacovig, P.; Comelli, G.; Baraldi, A.; Kiskinova, M.; Rosei, R., Orientational Anisotropy in Oxygen Dissociation on Rh(110). *Phys. Rev. B* **1999**, *60*, 7800-7803.
- 61. Schmid, M.; Leonardelli, G.; Tscheließnig, R.; Biedermann, A.; Varga, P., Oxygen Adsorption on Al(111): Low Transient Mobility. *Surf. Sci.* **2001**, *478*, L355-L362.
- 62. Rose, M. K.; Borg, A.; Dunphy, J. C.; Mitsui, T.; Ogletree, D. F.; Salmeron, M., Chemisorption of Atomic Oxygen on Pd(111) Studied by Stm. *Surf. Sci.* **2004**, *561*, 69-78.
- 63. Eric Klobas, J.; Schmid, M.; Friend, C. M.; Madix, R. J., The Dissociation-Induced Displacement of Chemisorbed O₂ by Mobile O Atoms and the Autocatalytic Recombination of O Due to Chain Fragmentation on Ag(110). *Surf. Sci.* **2014**, *630*, 187-194.
- 64. Brune, H.; Wintterlin, J.; Behm, R. J.; Ertl, G., Surface Migration of `Hot' Adatoms in the Course of Dissociative Chemisorption of Oxygen on Al(111). *Phys. Rev. Lett.* **1992**, *68*, 624-626.

- Brune, H.; Wintterlin, J.; Trost, J.; Ertl, G.; Wiechers, J.; Behm, R. J., Interaction of Oxygen with Al(111) Studied by Scanning Tunneling Microscopy. *J. Chem. Phys.* **1993**, *99*, 2128-2148.
- 66. Schintke, S.; Messerli, S.; Morgenstern, K.; Nieminen, J.; Schneider, W.-D., Far-Ranged Transient Motion of "Hot" Oxygen Atoms Upon Dissociation. *J. Chem. Phys.* **2001**, *114*, 4206-4209.
- 67. Wahnström, G.; Lee, A. B.; Strömquist, J., Motion of "Hot" Oxygen Adatoms on Corrugated Metal Surfaces. *J. Chem. Phys.* **1996**, *105*, 326-336.
- 68. Perron, N.; Pineau, N.; Arquis, E.; Rayez, J. C.; Salin, A., Adsorption of Atomic Oxygen on the Cu(100) Surface. *Surf. Sci.* **2005**, *599*, 160-172.
- 69. Sendner, C.; Groß, A., Kinetic Monte Carlo Simulations of the Interaction of Oxygen with Pt(111). *J. Chem. Phys.* **2007**, *127*, 014704.
- 70. Meyer, J.; Reuter, K., Electron–Hole Pairs During the Adsorption Dynamics of O_2 on Pd(100): Exciting or Not? *New J. Phys.* **2011**, *13*, 085010.
- 71. Komrowski, A. J.; Sexton, J. Z.; Kummel, A. C.; Binetti, M.; Weiße, O.; Hasselbrink, E., Oxygen Abstraction from Dioxygen on the Al(111) Surface. *Phys. Rev. Lett.* **2001**, *87*, 246103.

TOC graphic

